Mean-Square Bounded Consensus of Nonlinear Multi-Agent Systems with Time-Varying Delays via Impulsive Control Under Dual-Channel Stochastic Switching Deception Attacks

Abstract

This paper presents a novel dual-channel stochastic deceptive attack scheme, designed for multi-agent systems (MASs) utilizing directional network structures. The scheme compromises both sensor-controller (S-C) and controller-actuator (C-A) channels with distinct tampered signals during variable impulsive control intervals. To counter these attacks, an adaptive secure impulsive coordination strategy has been developed for a kind of non-linear Multi-Agent Systems with time-varying and dynamic switching capabilities. In this model, the stochastic selection of compromised channels obeys Bernoulli distributions. Based on Lyapunov's stability theorem, methods of matrix analysis, and linear matrix inequality techniques, adequate conditions are established to guarantee consensus in the mean-square sense with bounded errors for the system. Our key contributions include: (i) Novel criteria guaranteeing error-bounded consensus with explicit residual disagreement bounds; (ii) The first framework integrating dual-channel stochastic attacks with adaptive impulsive defense and time-varying delay functions; (iii) Analytical quantification of attack impacts on consensus precision. Two simulation cases are given to address the effectiveness of the derived results.

Keywords: Deception attacks, impulsive control, dual-channel stochastic switching, multi-agent systems, time-varying delays

1 Introduction

Recent years have witnessed substantial progress in cyber-physical networks, facilitating advanced coordination capabilities in domains including UAV formations [1, 2] and multi-robot systems [3]. Consequently, collective behaviors within these interconnected systems, particularly consensus and synchronization of multi-agent systems (MASs), have attracted substantial scholarly focus [4–6].

The theoretical foundation for analyzing such complex systems has been significantly advanced through stability analysis of dynamical systems which are subject to

time delays and impulses. Studies have investigated the exponential stability of nonlinear time-varying systems with delayed impulses and stochastic intensity [7], finite-time synchronization for fractional-order multiplex networks by using hybrid impulsive and quantized control [8], and novel stability criteria have been established for MASs with time-varying delay via advanced Lyapunov-Krasovskii functionals [9].

However, in practical implementations, MASs often operate in open-network environments that are vulnerable to various cybersecurity threats [10–12], significantly impacting their synchronization performance. Among these threats, denial-of-service (DoS) attacks [13] and deception attacks [14, 15] represent two predominant attack paradigms. Compared to DoS attacks that disrupt communication availability, deception attacks exhibit greater stealth by injecting malicious data into communication channels, posing more severe challenges to the consensus of MASs.

Existing research has made preliminary progress in addressing security challenges in MASs. Several studies have investigated deception attacks targeting individual channels, either sensor-controller (S-C) or controller-actuator (C-A) channels [16, 17], as well as bipartite synchronization under deception attacks [18]. Recent works have begun exploring hybrid threats combining deception with other cyber assaults [19]. However, current deception models predominantly focus on fixed attack patterns, overlooking the sophisticated stochastic switching strategies where adversaries dynamically alternate targets between S-C and C-A channels.

In real world, this research gap is particularly critical for MAS deployments. For instants, both swarm robotics and smart grids concurrently experience nonlinear interactions, limited communication resources, and coordinated cyber attacks that span multiple network channels. Beyond threat modeling, control protocol design remains pivotal. Diverse triggering mechanisms exist including periodic [20], event-based adaptive event-triggered, and self-triggered dynamic variants [21].

However, practical implementations will inevitably produce time-varying delays due to environmental noise, hardware limitations, and signal transmission constraints [22, 23], ect. These delays, particularly time-varying, can severely degrade synchronization performance which can cause triggering-time deviations and state inaccuracies. These phenomena have attracted much attention of many scholars. Some studies have been accomplished for MASs with time-varying delays [24–26]. Among these studies, many meaningful control methods have been proposed [22-26]. In many real situations, continuous control requires an ideal communication environment, which is often unavailable. To overcome this problem, impulsive control is proposed [27, 28]. Whereas, there are few reports have been given for MASs with time-varying delays if they encounter cyber threats. Hence, it is very necessary for us to seek for novel analytical frameworks and control protocols to solve these problems. Based on above discussions, existing approaches exhibit notable limitations. Specifically, the following critical challenges remain to beadequately addressed: (i) The dynamic and stochastic nature of multi-channel deception attacks, particularly in systems with random-switching attack patterns across channels; (ii) The compounded destabilizing effects from time-varying delays coupled with deception attacks; (iii) A lack of unified control frameworks incorporating impulsive control and adaptive security mechanisms to mitigate deception attacks while ensuring mean-square bounded consensus.

Within this study, the mean-square bounded consensus of a kind of non-linear MASs with time-varying delays under dual-channel ctochastic switching deception attacks will be discussed. Departing from prior focus on isolated nonlinear systems [29–32],this work will establish a theoretical framework for the mean-square bounded consensus with time-varying delays under stochastic deception attacks across dual communication channels. The core contributions are articulated as follows:

(1) A novel deception attack model is developed. In this new model, actuators encounter randomly alternating sensor-controller(S-C) and controller-actuator(C-A) deception signals across impulse intervals, generalizing prior single-channel frameworks.
(2) An adaptive switching-based secure impulsive control strategy is developed, utilizing Bernoulli distributions, linear matrix inequalities, and Lyapunov theory to establish synchronization criteria for mean-square bounded consensus.
(3) The impact of leader deception is analyzed, pioneering the study of leader-transmitted deception signals in open networks under dual-channel attacks with time-varying delays.

The paper is organised in the following manner. Preliminary symbols and graph-theoretic concepts are presented in section 2. The system model is established in section 3. Impulsive synchronisation of MASs subjected to dual-channel stochastic deception attacks with time-varying delays is investigated in section 4. Numerical experiments are conducted in section 5 to verify the theoretical findings. Final remarks are offered in section 6.

2 Preliminary

2.1 Mathematical Notation

Herein, $\mathbb{R}^n$ signifies the n-dimensional real Euclidean space; $\otimes$ denotes the Kronecker product; $P = P^\top \succ 0$ signifies a real symmetric positive-definite matrix; $\lambda_i(P)$ represents the i-th eigenvalue of matrix P, while $\lambda_{\max}(P)$ and $\lambda_{\min}(P)$ denote the largest eigenvalue and the smallest eigenvalue of P, respectively; $\rho(P)$ denotes the spectral radius of P; $\sigma_{\max}(P)$ denotes the largest singular value of P; $\|\cdot\|$ denotes the Euclidean 2-norm, so that for any vector $\|u\| = \sqrt{\sum_{i=1}^{n} u_i^2}$; and $\Pr\{\cdot\}$ denotes the probability that the associated random variable follows a Bernoulli distribution.

2.2 Graph Theory

The weighted directed graph is depicted by the triplet $\mathcal{G} = (\mathcal{A}, \mathcal{E}, R)$, where $\mathcal{A} = \{\tilde{A}_1, \tilde{A}_2, \ldots, \tilde{A}_N\}$ denotes the set of N nodes. An edge $e_{ij} \in \mathcal{E} \subseteq \mathcal{A} \times \mathcal{A}$ is denoted as (i, j), indicating that node j obtains information from node i. A directed path from node j to node i is a sequence of distinct edges $(j, b_1), (b_1, b_2), \ldots, (b_k, i)$ with distinct nodes b_k. The adjacency matrix $R = (a_{ij}) \in \mathbb{R}^{N\times N}$ satisfies $a_{ij} \geq 0$ if and only if edge $(j, i) \in \mathcal{E}$; if $a_{ij} = a_{ji}$ for all i, j, then R is symmetric. Graph Laplacian

$L = (\mathfrak{g}_{ij}) \in \mathbb{R}^{N\times N}$ is defined by

$$\mathfrak{g}_{ij} = -a_{ij}\ (i \neq j), \qquad \mathfrak{g}_{ii} = \sum_{\substack{j=1,\\ j\neq i}}^{N} a_{ij},$$

and satisfies $\sum_{j=1}^{N} \mathfrak{g}_{ij} = 0$ or every i.

3 Model Construction

In this section, our objective is to construct a model for lead-following MASs subject to dual-channel stochastic switching deception attacks, and design a control protocol to ensure the synchronization of the system.

3.1 Description of MASs with Time-varying delays

Consider a multi-agent system (MAS) composed of n followers, indexed by $i = 1, 2, \ldots, n$. The dynamics of the i-th follower are governed by the differential equation (1)

$$\begin{aligned} &\dot{x}_i(t) \\ &= \big[\mathscr{A}x_i(t) + \mathscr{A}_1(t)x(t-\tau(t)) + \mathscr{A}_2\phi(x_i(t-\tau(t))) + \hat{u}_i(t)\big]dt \\ &+ \mathscr{B}g(t, x_i(t), x(t-\tau(t))d\omega(t) \end{aligned} \tag{1}$$

where $x_i(t) \in \mathbb{R}^m$ is the state vector, $\mathscr{A}$, $\mathscr{A}_1$, $\mathscr{A}_2$ and $\mathscr{B}$ denote constant matrices. For every node $i \in \{1, \ldots, N\}$, the map $\phi\colon \mathbb{R} \to \mathbb{R}^N$ is assembled as $\phi\big(x_i(t)\big) = \big[\,\phi_1\big(x_i(t)\big),\ \phi_2\big(x_i(t)\big),\ \ldots,\ \phi_N\big(x_i(t)\big)\,\big]^\top$. $\hat{u}_i(t)$ embodies the control protocol described by (15). The function $\tau(t)$ denotes a time-varying delay that is inherent in the system.

The dynamic of the leader is supposed as following equation (2)

$$\begin{aligned} &\dot{l}_0(t) \\ &= \big[\mathscr{A}l_0(t) + \mathscr{A}_1(t)l(t-\tau(t)) + \mathscr{A}_2\phi(l_0(t-\tau(t))) + \hat{u}_i(t)\big]dt \\ &+ \mathscr{B}g(t, l_0(t), l(t-\tau(t))d\omega(t) \end{aligned} \tag{2}$$

To facilitate the analysis, the nonlinear function $\phi(\cdot)$ is assumed to comply with Hypothesis 1 and 2.

Hypothesis 1. For a vector-valued nonlinearity $\phi(\cdot)$, there exist constants $r_{ij} \geq 0$, defined for every $i = 1, \ldots, N$ and $j = 1, \ldots, n$, such that

$$\big|\phi_i(\mathfrak{p}_1) - \phi_i(\mathfrak{p}_2)\big| \leq \sum_{j=1}^{n} r_{ij}|\mathfrak{p}_{1,j} - \mathfrak{p}_{2,j}|, \quad \forall \mathfrak{p}_1, \mathfrak{p}_2 \in \mathbb{R}^n. \tag{3}$$

Hypothesis 2. The communication topology between the leader and all follower agents is connected, ensuring the existence of a directed path from the leader to every follower in the network.

For the convenience of later discussion, we firstly give the folowing Lemma 1, 2, 3 and 4.

Lemma 1. For any matrix $M \in \mathbb{R}^{n\times n}$ $(M \succ 0)$, a vector map $\psi : [a, b] \to \mathbb{R}^n$. With the quadratic functional defined as

$$\mathcal{J}(\psi) = \left(\int_a^b \psi(s)\, ds\right)^\top M \left(\int_a^b \psi(s)\, ds\right),$$

the inequality $\mathcal{J}(\psi) \leq (b-a)\int_a^b \psi^\top(s) M\psi(s)\, ds$ follows directly.

Lemma 2. [33] For any non-negative scalars $\hat{\alpha} \geq 0$ and $\hat{\beta} \geq 0$, and for a time-varying delay $\mathfrak{d}(t)$ satisfying $0 < \mathfrak{d}_1 \leq \mathfrak{d}(t) \leq \mathfrak{d}_2$, the following inequality is satisfied

$$\begin{aligned} &\frac{\hat{\alpha}}{\mathfrak{d}(t)-\mathfrak{d}_1} + \frac{\hat{\beta}}{\mathfrak{d}_2-\mathfrak{d}(t)} \\ &\geq \min\left\{\frac{3\hat{\alpha}+\hat{\beta}}{\mathfrak{d}_2-\mathfrak{d}_1}, \frac{\hat{\alpha}+3\hat{\beta}}{\mathfrak{d}_2-\mathfrak{d}_1}\right\}. \end{aligned} \tag{4}$$

Lemma 3.(Schur Complement Lemma[34]) For given constant matrices Ω_1, Ω_2 and Ω_3, where Ω_1 and Ω_2 are symmetric matrices, the following conditions are equivalent

(1) $\Omega = \begin{bmatrix} \Omega_1 & \Omega_3 \\ \Omega_3^T & \Omega_2 \end{bmatrix} < 0$;
(2) $\Omega_1 < 0$ and $\Omega_2 - \Omega_3^T\Omega_1^{-1}\Omega_3 < 0$;
(3) $\Omega_2 < 0$ and $\Omega_1 - \Omega_3\Omega_2^{-1}\Omega_3^T < 0$.

Lemma 4. (Halanay Inequality [35]) Let scalar map $\omega(t) \geq 0$ defined on $[t_0-\tau, \infty)$ and continuous on $[t_0, \infty)$. Suppose

$$D^+\omega(t) \leq -\tilde{\alpha}\omega(t) + \tilde{\beta}\omega(t-\tau), \quad t \geq t_0, \tag{5}$$

with $\tilde{\alpha} > \tilde{\beta} \geq 0$. Then

$$\omega(t) \leq \omega_0^\star \exp(-\lambda(t-t_0)), \tag{6}$$

where $\omega_0^\star = \sup_{t_0-\tau\leq\theta\leq t_0} \omega(\theta)$ and the unique $\lambda > 0$ satisfies

$$\lambda - \tilde{\alpha} + \tilde{\beta}e^{\lambda\tau} = 0 \tag{7}$$

.

Lemma 5. For any vectors $\varrho, \varsigma \in \mathbb{R}^n$, the inequality

$$\|\varrho + \varsigma\| \leq \|\varrho\| + \|\varsigma\|$$

holds. Assign $\varrho = e(u) - e(t)$, $\varsigma = e(t)$, and assume the Lipschitz condition $\|e(u) - e(t)\| \leq \mathbb{L} \cdot |u - t|$.

Then we have

$$\|e(u)\|^2 \leq 2\|e(t)\|^2 + 2\mathbb{L}^2|u - t|^2. \tag{8}$$

Proof

$$\begin{aligned} \|\varrho + \varsigma\|^2 &= (\varrho + \varsigma)^\top (\varrho + \varsigma) \\ &= \|\varrho\|^2 + \|\varsigma\|^2 + 2\varrho^\top \varsigma \\ &\leq \|\varrho\|^2 + \|\varsigma\|^2 + 2\|\varrho\| \cdot \|\varsigma\| \\ &\leq \|\varrho\|^2 + \|\varsigma\|^2 + \left(\|\varrho\|^2 + \|\varsigma\|^2\right) \\ &= 2\|\varrho\|^2 + 2\|\varsigma\|^2. \end{aligned} \tag{9}$$

Substituting the above choices for ϱ and ς, together with the given Lipschitz bound, yields the desired inequality

$$\|e(u)\|^2 \leq 2\|e(t)\|^2 + 2\mathbb{L}^2|u - t|^2. \tag{10}$$

□

Lemma 6.[36] Consider a positive-definite matrix $\mathcal{P} \succ 0$,$\mathcal{P} = U\Lambda U^\mathsf{T}$ with $\varkappa = \text{diag}(\varkappa_1, \ldots, \varkappa_n)$. For any vector $\hat{\xi}$, the following inequality holds:

$$\varkappa_{\min}(\mathcal{P})\|\hat{\xi}\|^2 \leq \hat{\xi}^\mathsf{T}\mathcal{P}\hat{\xi} \leq \varkappa_{\max}(\mathcal{P})\|\hat{\xi}\|^2. \tag{11}$$

Remark 1 In contrast to the synchronous attack model presented in [38], this paper introduces a time-varying delay function into the deception attack framework, significantly enhancing its applicability to real-world scenarios. As indicated in (1) and (2), multiple adversaries in our model are capable of independently targeting different communication channels with distinct attack strategies. Moreover, attack sequences can differ across communication channels, allowing adversaries to implement distributed attack strategies tailored to specific targets. The inclusion of a time-varying delay function more accurately captures the dynamic nature of practical networked environments, thereby strengthening the robustness of the security mechanism. Consequently, the node-based event-triggered approach adopted in [26] becomes inadequate under these conditions, necessitating the design of a channel-based event-triggered mechanism that explicitly accounts for time-varying delays.

3.2 S-C Deception Attacks

In MASs, if the sensor-controller channel is subjected to deception attacks, and the attack mode is extended from targeting individual agents to disrupt system-wide communication links, then agents will receive false signals from their neighbors. As a result, incorrect data will be transfered among agents. In this situation, consensus of MASs will become to be difficult. To solve this problem, an adaptive secure impulsive consensus control protocol is designed as following (12)

$$\tilde{u}_i(t) = b_k \sum_{k=1}^{\infty} \xi_i(t)\delta(t - t_k), \tag{12}$$

where

$$\xi_i(t) = \sum_{j=1}^{N} \left(-\mathcal{L}_{ij} x_j(t) + \beta_{ij}(t)\xi_{ij}(t)\right) - c_i \left(x_i(t) - \ell(t)\right). \tag{13}$$

$\mathcal{L}ij$ denotes elements of the Laplacian matrix. The adaptive impulse gain $b_k > 0$ ($k \in \mathbb{Z}^+$) dynamically mitigates attack impacts, while $c_i \geq 0$ defines the pinning gain. Impulse timing is governed by the Dirac delta function $\delta(\cdot)$. On S-C channels, deception signals $\xi(t) = \left[\xi_1(t)^\mathsf{T}, \ldots, \xi_N(t)^\mathsf{T}\right]^\mathsf{T} \in \mathbb{R}^{Nn}$ satisfy $\xi_i(t) = \left[\xi_{i1}(t)^\mathsf{T}, \ldots, \xi_{iN}(t)^\mathsf{T}\right]^\mathsf{T} \in \mathbb{R}^n$ with $\xi_{ij}(t) \in \mathbb{R}^n$. The stochastic switching variable $\beta_{ij}(t) \in 0, 1$ follows a Bernoulli distribution whose probability mass function is

$$\Pr\left(\beta_{ij}(t) = 1\right) = \lambda_{ij}, \quad \Pr\left(\beta_{ij}(t) = 0\right) = 1 - \lambda_{ij}, \tag{14}$$

where $\lambda_{ij} \in [0, 1)$ is the attack probability.

Hypothesis 3. The stochastic variables $\beta_{ij}(t)$ for $(i, j) \in \varepsilon_G$, and $\alpha_i(t)$ are mutually independent.

3.3 S-C and C-A Switching Deception Attacks

This paper investigates a sophisticated cyber-attack framework within networked control systems, involving dual-channel deception attacks:

(1) Edge-based deception attacks compromise sensor-controller (S-C) channels (Section 3.2);
(2) Stochastic switching deception attacks target both S-C and controller-actuator (C-A) links, with adversarial signals alternating across impulse instants(Figure 1).

We design an adaptive switching secure impulsive protocol

$$\hat{u}_i(t) = \sum_{k=0}^{\infty} \left[\alpha_i(t)\zeta_i(t) + (1 - \alpha_i(t))\tilde{u}_i(t)\right] \delta(t - t_k), \tag{15}$$

where $\zeta(t) = (\zeta_1(t), \ldots, \zeta_N(t)) \in \mathbb{R}^{Nn}$ denotes the deception signals injected into C-A channels. The impulse sequence $\{t_k \mid k \in \mathbb{Z}^+\}$ adheres to $0 \leq t_k < t_{k+1}$ with $\upsilon_{\min} = \inf_k\{t_k - t_{k-1}\}$ and $\upsilon_{\max} = \sup_k\{t_k - t_{k-1}\}$. The stochastic variable distributed by Bernoulli $\alpha_i(t)$ characterizes the success of the attack

$$\Pr\{\alpha_i(t) = k\} = \begin{cases} \kappa, & k = 1 \quad \text{(attack successful)}, \\ 1 - \kappa, & k = 0 \quad \text{(attack failed)}. \end{cases} \tag{16}$$

Remark 2 The novel dual-channel stochastic switching deception attack strategy is illustrated as Figure 1. The key aspect that differentiates this model from existing dual-channel deception attack frameworks, such as that presented in [37], is the incorporation of a time-varying delay function $\tau(t)$. Developed within the setting of nonlinear multi-agent systems with time-varying delays, this extension significantly improves the practical applicability and adaptive capacity of the attack strategy.

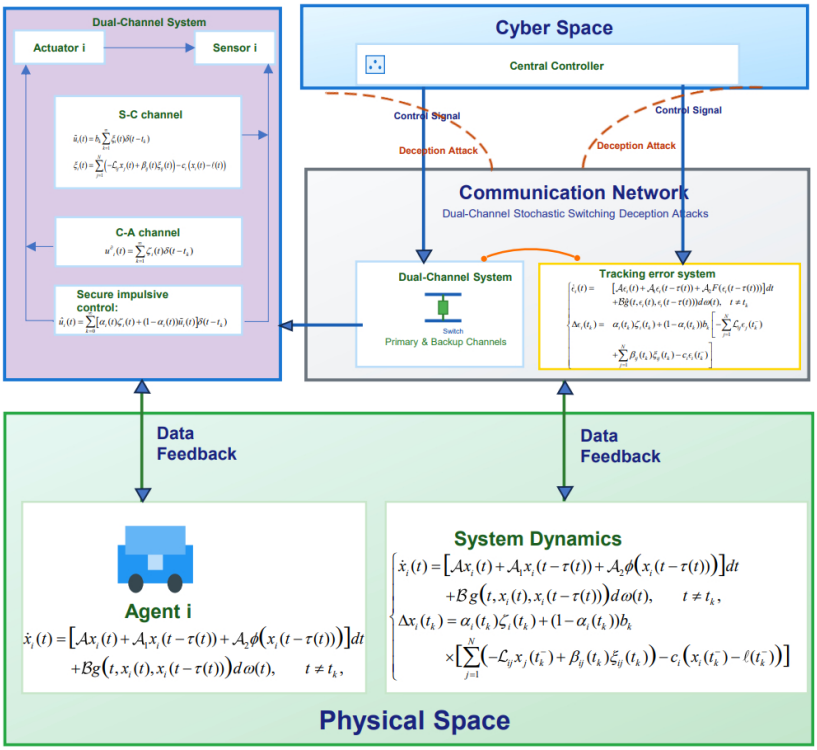

Fig. 1 MASs system architecture with dual-channel stochastic switching under deception attacks.

In contrast to the model in [38], the stochastic variable restricts attacks to both channels simultaneously or to no channel at all, our approach provides enhanced flexibility through dynamic switching between channels. Specifically, when $\alpha_i(\tau) = 0$, only the sensor-to-controller (S-C) channel is compromised; otherwise, the attack switches to the controller-to-actuator (C-A) channel. The proposed deception attack model offers several tactical and practical advantages:

(1) It reduces energy consumption by utilizing single-channel resources to achieve disruptive effects comparable to dual-channel attacks.
(2) The incorporation of time-varying delay increases uncertainty and improves stealth.
(3) The combination of dynamic switching and time-varying delays enhances adaptability and raises the success rate of attacks.

As a result, this refined attack framework poses a more significant challenge to the synchronization of nonlinear MASs and more accurately reflects real-world attack scenarios, where time-varying delays and switching behaviors are frequently observed.

3.4 Tracking error system

The mean-square bounded synchronization requires continual observation of every follower and the leader. Based on (1), (2), (12)and (15), it can be concluded that

$$\begin{cases} \dot{x}_i(t) = \big[\mathscr{A}x_i(t) + \mathscr{A}_1 x_i(t-\tau(t)) + \mathscr{A}_2\phi\big(x_i(t-\tau(t))\big)\big]\,dt \\ \qquad\quad + \mathscr{B}\,g\big(t, x_i(t), x_i(t-\tau(t))\big)\,d\omega(t), \qquad t \neq t_k, \\ \Delta x_i(t_k) = \alpha_i(t_k)\zeta_i(t_k) + (1-\alpha_i(t_k))b_k \\ \qquad\quad \times\Big[\sum_{j=1}^{N}\Big(-\mathcal{L}_{ij}x_j(t_k^-) + \beta_{ij}(t_k)\xi_{ij}(t_k)\Big) - c_i\big(x_i(t_k^-) - \ell(t_k^-)\big)\Big], \end{cases}$$

where $\Delta x_i(t_k) = x_i(t_k^+) - x_i(t_k^-)$, $x_i(t_k^+) = \lim_{\omega\to 0^+} x_i(t_k+\omega)$,and $x_i(t_k^-) = \lim_{\omega\to 0^-} x_i(t_k+\omega)$. Define the synchronization error $\epsilon_i(t) = x_i(t) - l_0(t)$, and $\hat{g}(t,\epsilon_i,\epsilon_i(t-\tau)) = g(t,x_i,x_i(t-\tau)) - g(t,l_0,l_0(t-\tau))$.Then the error system is described as following equation (17)

$$\begin{cases} \dot{\epsilon}_i(t) = [\mathscr{A}\epsilon_i(t) + \mathscr{A}_1\epsilon_i(t-\tau(t)) + \mathscr{A}_2 F(\epsilon_i(t-\tau(t)))]\,dt \\ \qquad\quad + \mathscr{B}\hat{g}(t,\epsilon_i(t),\epsilon_i(t-\tau(t)))d\omega(t), \quad t \neq t_k \\ \Delta\epsilon_i(t_k) = \alpha_i(t_k)\zeta_i(t_k) + (1-\alpha_i(t_k))b_k\Big[-\sum_{j=1}^{N}\mathcal{L}_{ij}\epsilon_j(t_k^-) \\ \qquad\quad + \sum_{j=1}^{N}\beta_{ij}(t_k)\xi_{ij}(t_k) - c_i\epsilon_i(t_k^-)\Big]. \end{cases} \tag{17}$$

In equation (17), the nonlinear error function is

$$F\big(\epsilon_i(t-\tau(t))\big) = \phi\big(\epsilon_i(t-\tau(t)) + l_0(t-\tau(t))\big) - \phi\big(l_0(t-\tau(t))\big), \quad t \neq t_k,$$

with the jump condition

$$\Delta\epsilon_i(t_k) = \epsilon_i(t_k^+) - \epsilon_i(t_k^-), \quad \epsilon_i(t_k^+) = \lim_{h\to 0^+}\epsilon_i(t_k+h), \quad \epsilon_i(t_k^-) = \lim_{h\to 0^-}\epsilon_i(t_k+h).$$

Rewriting the error dynamics, the Kronecker product form of equation (17) can be denoted as following equation (18)

$$\begin{cases} \dot{\epsilon}(t) = & \Big[(I_N \otimes \mathscr{A})\,\epsilon(t) + (I_N \otimes \mathscr{A}_1)\,\epsilon(t-\tau(t)) \\ & \quad +(I_N \otimes \mathscr{A}_2)\,F\big(\epsilon(t-\tau(t))\big)\Big]dt + \mathbf{G}(t)\,d\mathbf{W}(t), \qquad t \neq t_k, \\ \epsilon(t_k) = & \Big[I_{Nn} - b_k\big((I_N - \Lambda(t_k))(L+C) \otimes I_n\big)\Big]\epsilon(t_k^-) \\ & \quad +\big(\Lambda(t_k) \otimes I_n\big)\zeta(t_k) \\ & \quad +b_k\big((I_N - \Lambda(t_k)) \otimes I_n\big)\Xi(t_k), \qquad t = t_k, \end{cases} \tag{18}$$

where the vector $\epsilon(t) = \big(\epsilon_1^\top(t), \epsilon_2^\top(t), \cdots, \epsilon_N^\top(t)\big)^\top \in \mathbb{R}^{Nn}$ represents the state error of N followers relative to the leader. The diagonal matrix $\Lambda(t_k) = \operatorname{diag}(\alpha_1(t_k), \alpha_2(t_k), \cdots, \alpha_N(t_k)) \in \mathbb{R}^{N\times N}$ is the channel-switching matrix with Bernoulli entries ($\Pr(\alpha_i(t_k) = 1) = \kappa$). The matrix $H = L + C$, where $C = \operatorname{diag}(c_1, c_2, \cdots, c_N)$ is the pinning gain matrix. Additionally, $\Xi(t_k) = \Big(\big(\sum_j \beta_{1j}(t_k)\xi_{1j}(t_k)\big)^\top, \cdots, \big(\sum_j \beta_{Nj}(t_k)\xi_{Nj}(t_k)\big)^\top\Big)^\top \in \mathbb{R}^{Nn}$ denotes the S-C deception attack vector, and $\zeta(t_k) = \big(\zeta_1^\top(t_k), \cdots, \zeta_N^\top(t_k)\big)^\top \in \mathbb{R}^{Nn}$ represents the C-A deception attack vector. The adaptive impulse gain is denoted by $b_k > 0$,

$$\mathbf{G}(t) = \begin{bmatrix} \mathscr{B}\hat{g}_1(t) & & \mathbf{0} \\ & \ddots & \\ \mathbf{0} & & \mathscr{B}\hat{g}_N(t) \end{bmatrix} \in \mathbb{R}^{N\times N},$$

and

$$\mathbf{W}(t) = \big[\omega_1(t), \ldots, \omega_N(t)\big]^\top \in \mathbb{R}^N.$$

Hypothesis 4. The adversarial signal remains bounded such that

$$\|\xi(t_k)\|_2 \leq \bar{\xi},$$

in which $\bar{\xi}$ denotes a known positive bound. Owing to the stochastic nature of the attack, this research will investigate the mean-square bounded consensus within MASs.

Definition 1 The multi-agent system (1) and the leader system (2) are said to achieve mean-square bounded synchronization within a prescribed error bound under exogenous disturbances if there exist a compact set $\mathcal{C} \subset \mathbb{R}^{n\times N}$ and a constant $R > 0$ such that, for all initial states $x_i(0), s(0) \in \mathbb{R}^n$,

$$\limsup_{t\to\infty} \mathbb{E}\big[\|\epsilon(t)\|\big] \leq R,$$

i.e., the synchronization error $e(t)$ ultimately enters and remains within the set

$$\mathcal{C} = \Big\{e \in \mathbb{R}^{n\times N} \;\Big|\; \mathbb{E}\big[\|\epsilon\|\big] \leq R\Big\}.$$

Definition 2 Define the vector $y(t) \in \mathbb{R}^n$ such that it meets

$$y(t)dt = d\epsilon(t), \quad y(t) = \phi(t), \quad t \in [-\tau_M, 0]. \tag{19}$$

According to the Leibniz–Newton identity (Lemma 5), we derive:

$$\int_{t-\tau(t)}^{t} y(s)ds = \epsilon(t) - \epsilon(t - \tau(t)).$$

4 Secure Consensus Analysis

In this section, sufficient conditions will be derived to ensure mean-square bounded consensus of MAS (1).

Construct the Lyapunov-Krasovskii functional as follows

$$\mathscr{V}(\epsilon(t)) = \mathscr{V}_1(\epsilon(t)) + \mathscr{V}_2(\epsilon(t)) + \mathscr{V}_3(\epsilon(t)). \tag{20}$$

Here, $\epsilon(t)$ denotes the solution of the error system (17). Consider symmetric positive definite matrices P, S_1, Q_j, R_j and positive scalars $\mu > 0$. Along the solution trajectory, we define:

$$\mathscr{V}_1(\epsilon(t)) = \epsilon^T(t)P\epsilon(t) + \int_{t-\tau(t)}^{t} \epsilon^T(s)S_1\epsilon(s)ds \tag{21}$$

$$\mathscr{V}_2(\epsilon(t)) = \sum_{j=1}^{m} \int_{-\tau_j}^{-\tau_{j-1}} \epsilon^T(t+s)Q_j\epsilon(t+s)ds \tag{22}$$

$$\mathscr{V}_3(\epsilon(t)) = \sum_{j=1}^{m} \delta_j \int_{-\tau_j}^{-\tau_{j-1}} \int_{t+\theta}^{t} \dot{\epsilon}^T(s)R_j\dot{\epsilon}(s)dsd\theta \tag{23}$$

where $P > 0$, $S_1 > 0$, $Q_j > 0$, $R_j > 0$ $(j = 1, \ldots, m)$, $\delta_j = \tau_j - \tau_{j-1}$, and the matrix inequality

$$\begin{bmatrix} Q_j & 0 \\ * & R_j \end{bmatrix} > 0$$

ensures the positive definiteness of $\mathscr{V}_3$.

Lemma 7. The expected value of $\mathscr{V}_1(\epsilon(t))$ satisfies, $\widetilde{\beta}$ is related to the probability of communication failure, θ and ξ are related to noise bounds, ε is a positive scalar parameter, κ is an upper bound coefficient for the integral term.

$$\mathbb{E}\{\mathscr{V}_1(\epsilon(t_k^+))\} \leq c_1\mathbb{E}[\mathscr{V}(t_k^-)] + d_1 \tag{24}$$

where

$$\begin{aligned} c_1 &= \mu_1 + \widetilde{\beta}\varepsilon + \kappa, \\ d_1 &= \widetilde{\beta}\theta\xi\left(\varepsilon^{-1} + 1\right). \end{aligned}$$

Proof According to (18), the system state experiences a jump governed by

$$\epsilon(t_k^+) = \mathbb{M}(t_k)\,\epsilon(t_k^-) + \mathbb{G}(t_k), \tag{25}$$

where

$$\mathbb{M}(t_k) = I_{Nn} - b_k\big[\big(I_N - \Lambda(t_k)\big)(L + C) \otimes I_n\big],$$

and

$$\mathbb{G}(t_k) = \big(\Lambda(t_k) \otimes I_n\big)\zeta(t_k) + b_k\big[\big(I_N - \Lambda(t_k)\big) \otimes I_n\big]\Xi(t_k).$$

Owing to the impulse-time dynamics (25), the expected value of the quadratic form $\epsilon^T(t_k^+)P\epsilon(t_k^+)$ admits the exact decomposition

$$\begin{aligned}\mathbb{E}\{\mathscr{V}_1(\epsilon(t_k^+))\} = {} & \epsilon^T(t_k^-)\,\mathbb{E}\big[\mathbb{M}^T(t_k)P\mathbb{M}(t_k)\big]\,\epsilon(t_k^-) \\ & + 2\epsilon^T(t_k^-)\,\mathbb{E}\big[\mathbb{M}^T(t_k)P\mathbb{G}(t_k)\big] \\ & + \mathbb{E}\big[\mathbb{G}^T(t_k)P\mathbb{G}(t_k)\big] + I(t_k^-),\end{aligned} \tag{26}$$

where

$$I(t_k^-) = \mathbb{E}\left[\int_{t_k-\tau(t_k)}^{t_k} \epsilon^T(s)S_1\epsilon(s)\,ds\right].$$

To establish an upper bound for $\mathbb{E}\{\mathscr{V}_1(\epsilon(t_k^+))\}$, we analyze each term in (26) separately. For the first term, we have

$$\mathbb{E}[\epsilon^T(t_k^-)\mathbb{M}^T(t_k)P\mathbb{M}(t_k)\epsilon(t_k^-)] \le \mu_1\mathbb{E}[\mathscr{V}(t_k^-)] \tag{27}$$

where

$$\mu_1 = \rho\left(I_N + c^2(1-\widetilde{\beta})H^TH - c(1-\widetilde{\beta})(H + H^T)\right),$$

and $\rho(\cdot)$ denotes the spectral radius.

For the second terms, we obtain

$$2\mathbb{E}[\epsilon^T(t_k^-)\mathbb{M}^T(t_k)P\mathbb{G}(t_k)] \le \widetilde{\beta}\varepsilon\mathbb{E}[\mathscr{V}(t_k^-)] + \widetilde{\beta}\varepsilon^{-1}\theta\xi. \tag{28}$$

For the third term, we have

$$\mathbb{E}[\mathbb{G}^T(t_k)P\mathbb{G}(t_k)] \le \widetilde{\beta}\theta\xi. \tag{29}$$

For the fourth term $I(t_k^-)$, we establish the upper bound condition

$$I(t_k^-) \le \kappa\mathbb{E}[V(t_k^-)]. \tag{30}$$

Combining the estimates (27)-(30), we obtain

$$\mathbb{E}\{\mathscr{V}_1(\epsilon(t_k^+))\} \le \left(\mu_1 + \widetilde{\beta}\varepsilon + \kappa\right)\mathbb{E}[\mathscr{V}(t_k^-)] + \widetilde{\beta}\theta\xi\left(\varepsilon^{-1} + 1\right). \tag{31}$$

Then inequality (31) can be written compactly as following form (32)

$$\mathbb{E}\{\mathscr{V}_1(\epsilon(t_k^+))\} \le \hat{\mu}\mathbb{E}[\mathscr{V}(t_k^-)] + \hat{m} \tag{32}$$

where

$$\begin{aligned} c_1 &= \mu_1 + \widetilde{\beta}\varepsilon + \kappa, \\ d_1 &= \widetilde{\beta}\theta\xi\left(\varepsilon^{-1} + 1\right). \end{aligned}$$

□

Lemma 8. Under the assumption that the state trajectory is Lipschitz continuous with constant L, i.e., $\|\epsilon(u) - \epsilon(t)\| \leq L|u - t|$ for $u \in [t - \tau_j, t - \tau_{j-1}]$, the expected value of $\mathscr{V}_2(\epsilon(t))$ satisfies

$$\mathbb{E}[\mathscr{V}_2(\epsilon(t))] \leq c_2 \mathbb{E}[\epsilon^T(t) P \epsilon(t)] + d_2 \tag{33}$$

where

$$c_2 = \sum_{j=1}^{m} \frac{2\lambda_{\max}(Q_j)(\tau_j - \tau_{j-1})}{\lambda_{\min}(P)}, \tag{34}$$

$$d_2 = \sum_{j=1}^{m} 2\lambda_{\max}(Q_j) L^2 \tau_{\max}^2 (\tau_j - \tau_{j-1}), \tag{35}$$

and $\tau_{\max} = \max_j \tau_j$.

Proof Using Lemma 5, we have $\|\epsilon(u)\|^2 \leq 2\|\epsilon(t)\|^2 + 2L^2|u - t|^2$. Since $|u - t| \leq \tau_{\max}$, it follows that

$$\|\epsilon(u)\|^2 \leq 2\|\epsilon(t)\|^2 + 2L^2\tau_{\max}^2. \tag{36}$$

Then,

$$\epsilon^T(u) Q_j \epsilon(u) \leq \lambda_{\max}(Q_j) \|\epsilon(u)\|^2 \leq \lambda_{\max}(Q_j) \left(2\|\epsilon(t)\|^2 + 2L^2\tau_{\max}^2\right). \tag{37}$$

Integrating over u from $t - \tau_j$ to $t - \tau_{j-1}$,

$$\int_{t-\tau_j}^{t-\tau_{j-1}} \epsilon^T(u) Q_j \epsilon(u) du \leq \lambda_{\max}(Q_j) \left(2\|\epsilon(t)\|^2 + 2L^2\tau_{\max}^2\right) (\tau_j - \tau_{j-1}). \tag{38}$$

From Lemma 6, $\|\epsilon(t)\|^2 \leq \frac{1}{\lambda_{\min}(P)} \epsilon^T(t) P \epsilon(t)$. Therefore,

$$\begin{aligned} &\int_{t-\tau_j}^{t-\tau_{j-1}} \epsilon^T(u) Q_j \epsilon(u) du \\ &\leq \frac{2\lambda_{\max}(Q_j)(\tau_j - \tau_{j-1})}{\lambda_{\min}(P)} \epsilon^T(t) P \epsilon(t) \\ &\quad + 2\lambda_{\max}(Q_j) L^2 \tau_{\max}^2 (\tau_j - \tau_{j-1}). \end{aligned} \tag{39}$$

Summing over j and taking expectation, the result can be yielded. □

Lemma 9. If there exists $L_d > 0$ such that $\|\dot{\epsilon}(s)\|^2 \leq L_d \|\epsilon(t)\|^2$ for $s \in [t + \theta, t]$ with $\theta \in [-\tau_j, -\tau_{j-1}]$, then the expected value of $\mathscr{V}_3(\epsilon(t))$ satisfies

$$\mathbb{E}[\mathscr{V}_3(\epsilon(t))] \leq c_3 \mathbb{E}[\epsilon^T(t) P \epsilon(t)] \tag{40}$$

where

$$c_3 = \frac{1}{\lambda_{\min}(P)} \sum_{j=1}^{m} \delta_j \lambda_{\max}(R_j) L_d \cdot \frac{1}{2} (\tau_j^2 - \tau_{j-1}^2). \tag{41}$$

Proof From the assumption that $\|\dot{\epsilon}(s)\|^2 \leq L_d\|\epsilon(t)\|^2$, we have

$$\begin{aligned}\dot{\epsilon}^T(s)R_j\dot{\epsilon}(s) &\leq \lambda_{\max}(R_j)\|\dot{\epsilon}(s)\|^2 \\ &\leq \lambda_{\max}(R_j)L_d\|\epsilon(t)\|^2.\end{aligned} \tag{42}$$

Consider the inner integral

$$\begin{aligned}&\int_{t+\theta}^{t} \dot{\epsilon}^T(s)R_j\dot{\epsilon}(s)ds \\ &\leq \int_{t+\theta}^{t} \lambda_{\max}(R_j)L_d\|\epsilon(t)\|^2 ds \\ &= \lambda_{\max}(R_j)L_d\|\epsilon(t)\|^2|\theta|,\end{aligned} \tag{43}$$

where $|\theta| = -\theta$ since $\theta \in [-\tau_j, -\tau_{j-1}]$ is negative. Substituting (43) into the expression for $V_3(\epsilon(t))$,

$$\begin{aligned}\mathscr{V}_3(\epsilon(t)) &\leq \sum_{j=1}^{m}\delta_j \int_{-\tau_j}^{-\tau_{j-1}} \lambda_{\max}(R_j)L_d\|\epsilon(t)\|^2(-\theta)d\theta \\ &= \sum_{j=1}^{m}\delta_j\lambda_{\max}(R_j)L_d\|\epsilon(t)\|^2 \int_{-\tau_j}^{-\tau_{j-1}}(-\theta)d\theta.\end{aligned} \tag{44}$$

Evaluate the integral

$$\int_{-\tau_j}^{-\tau_{j-1}}(-\theta)d\theta = \int_{\tau_{j-1}}^{\tau_j} u du = \frac{1}{2}(\tau_j^2 - \tau_{j-1}^2), \tag{45}$$

where $u = -\theta$.

Thus

$$\mathscr{V}_3(\epsilon(t)) \leq \sum_{j=1}^{m}\delta_j\lambda_{\max}(R_j)L_d\|\epsilon(t)\|^2 \cdot \frac{1}{2}(\tau_j^2 - \tau_{j-1}^2). \tag{46}$$

Using the property of positive definite matrices that $\|\epsilon(t)\|^2 \leq \frac{1}{\lambda_{\min}(P)}\epsilon^T(t)P\epsilon(t)$, we obtain

$$\begin{aligned}\mathscr{V}_3(\epsilon(t)) &\leq \left(\frac{1}{\lambda_{\min}(P)}\sum_{j=1}^{m}\delta_j\lambda_{\max}(R_j)L_d \cdot \frac{1}{2}(\tau_j^2 - \tau_{j-1}^2)\right)\epsilon^T(t)P\epsilon(t) \\ &= c_3\epsilon^T(t)P\epsilon(t).\end{aligned} \tag{47}$$

Taking expectation on both sides and using the linearity of expectation

$$\mathbb{E}[\mathscr{V}_3(\epsilon(t))] \leq c_3\mathbb{E}[\epsilon^T(t)P\epsilon(t)]. \tag{48}$$

□

Remark 3 The bounds obtained in Lemmas 7–9 are instrumental in verifying the stochastic stability of the error system. By synthesizing these three auxiliary results we arrive at the pivotal inequality

$$\mathbb{E}[V(\epsilon(t))] \leq \mu\,\mathbb{E}\Big[\epsilon^\top(t)P\epsilon(t)\Big] + m, \tag{49}$$

which coincides with (75). μ and m are specified in Theorem 1. Consequently, Lemmas 7–9 jointly deliver sufficient conditions that enable the conclusion of Theorem 1.

Theorem 1 *Given that Hypothesis 1-4 are satisfied, the error system (17) achieves exponential convergence into the region*

$$\mathcal{C} = \left\{ \epsilon(t) \in \mathbb{R}^{n \times N} \;\middle|\; \mathbb{E}\left[\|\epsilon(t)\|\right] < \sqrt{\frac{m}{\eta(1-\mu\epsilon^{-\lambda_i h})}} \right\}$$

provided that conditions (H1) to (H6) are all met.

(H1) $\eta I \preceq P$ *for some* $\eta > 0$ *and positive definite* P

(H2) $0 < \mu < 1$

(H3) $r = \mu e^{-\lambda_i h} < 1$ *for all* i

(H4) $\alpha_i = \lambda_i - \dfrac{\ln \mu}{h} > 0$ *for all* i

(H5) $\epsilon^{-\alpha h_2} > \mu$

(H6) One may select a symmetric positive-definite matrix, denoted by $P_1 \succ 0$*, along with positive scalars* $\alpha > 0$*,* $\beta > 0$*, and a symmetric negative–semi–definite matrix* $\Theta \preceq 0$ *such that*

$$\begin{bmatrix} \hat{\Lambda} + \Sigma + \Theta & P_1\Gamma_1 \\ \Gamma_1^{\mathsf{T}} P_1 & -P_1 \end{bmatrix} \preceq 0, \tag{50}$$

where

$$\Sigma = \operatorname{diag}\big(-\alpha P_1,\ \beta P_1,\ 0, \ldots, 0\big). \tag{51}$$

The parameters μ *and* m *embedded in* $\hat{\Lambda}$ *are given by*

$$\mu = c_1 + c_2 + c_3, m = d_1 + d_2,$$

where c_1 *and* d_1 *are extracted from the upper bound on* $\mathbb{E}[V_1(e(t))]$ *in Lemma 7 ,* c_2 *and* d_2 *are given by Lemma 8,* c_3 *is provided by Lemma 9.*

Remark 4 The following provides an explanation for (H6).

Define an augmented state vector that captures both current and delayed states:

$$\xi^{\mathsf{T}}(t) = \big[x^{\mathsf{T}}(t),\ x^{\mathsf{T}}(t-\tau_1),\ x^{\mathsf{T}}(t-\tau_2),\ \ldots,\ x^{\mathsf{T}}(t-\tau_n),\ \dot{x}^{\mathsf{T}}(t)\big]. \tag{52}$$

The matrix Γ_1 captures the system's dynamic structure:

$$\Gamma_1 = \big[\mathscr{A},\ \mathscr{A}_1,\ 0,\ 0,\ \ldots,\ 0\big], \tag{53}$$

where $\mathscr{A}$ and $\mathscr{A}_1$ are the system matrices from the state-space representation

$$\begin{aligned} \mathrm{d}x_i(t) = &\big[\mathscr{A}x_i(t) + \mathscr{A}_1 x_i\big(t-\tau(t)\big) + \mathscr{A}_2\phi\big(x_i\big(t-\tau(t)\big)\big)\big]\mathrm{d}t \\ &+ \mathscr{B}\, g\big(t, x_i(t), x_i\big(t-\tau(t)\big)\big)\,\mathrm{d}\omega(t). \end{aligned} \tag{54}$$

The terms in the Lyapunov functional can be expressed as

$$\alpha\mathscr{V}(x(t),t) + \beta\mathscr{V}(x(t-\tau_k),t) = \xi^{\mathsf{T}}(t)\Sigma_1\xi(t), \tag{55}$$

where

$$\Sigma_1 = \operatorname{diag}(\alpha P_1,\ \beta P_1,\ 0, \ldots, 0). \tag{56}$$

Exploiting the Schur complement equivalence, the original linear matrix inequality given in hypothesis (H6) can be recast as the following equivalent reformulation

$$\hat{\Lambda} + \Gamma_1^{\mathsf{T}} P_1 \Gamma_1 + \Sigma + \Theta \preceq 0. \tag{57}$$

The negative semi-definite matrix Θ is designed to bound these perturbations:

$$-\max\{3W_{k1}+W_{k2},\ W_{k1}+3W_{k2}\} \le \xi^{\mathsf{T}}(t)\Theta\xi(t). \tag{58}$$

This leads to the inequality

$$\begin{aligned}&\xi^{\mathsf{T}}(t)\big(\hat{\Lambda}+\Gamma_1^{\mathsf{T}}P_1\Gamma_1\big)\xi(t)-\max\{3W_{k1}+W_{k2},\ W_{k1}+3W_{k2}\}\\&\le \xi^{\mathsf{T}}(t)\big(\hat{\Lambda}+\Gamma_1^{\mathsf{T}}P_1\Gamma_1+\Theta\big)\xi(t).\end{aligned} \tag{59}$$

Substituting the LMI condition yields

$$\begin{aligned}\dot{\mathscr{V}}(t) &\le \xi^{\mathsf{T}}(t)\big(\hat{\Lambda}+\Gamma_1^{\mathsf{T}}P_1\Gamma_1+\Theta\big)\xi(t)\\&\le -\xi^{\mathsf{T}}(t)\Sigma\xi(t),\end{aligned} \tag{60}$$

which simplifies to

$$\dot{\mathscr{V}}(t) \le -\alpha\, x^{\mathsf{T}}(t)P_1x(t)+\beta\, x^{\mathsf{T}}(t-\tau_k)P_1x(t-\tau_k). \tag{61}$$

Under the condition that $x^{\mathsf{T}}(t-\tau_k)P_1x(t-\tau_k) \le \delta\, x^{\mathsf{T}}(t)P_1x(t)$ for some $\delta>0$, we obtain

$$\dot{\mathscr{V}}(t) \le -(\alpha-\beta\delta)\mathscr{V}(x(t),t) < 0, \tag{62}$$

This strict inequality guarantees exponential convergence of the error dynamics when $\alpha > \beta\delta$.

The LMI approach in (H6) thus provides a computationally verifiable condition that ensures the Lyapunov functional decreases exponentially along system trajectories, guaranteeing robust stability despite time-varying delays and uncertainties.

Proof According to Itô's differential formula, the error trajectory is given by

$$d\mathscr{V}(\epsilon(t)) = \mathcal{L}\mathscr{V}(\epsilon(t))dt + 2\epsilon^T(t)PB\hat{g}(t)d\omega(t), \tag{63}$$

where the infinitesimal operator $\mathcal{L}\mathscr{V}(e(t))$ is defined as

$$\mathcal{L}\mathscr{V}(\epsilon(t)) = \mathcal{L}\mathscr{V}_1(\epsilon(t)) + \mathcal{L}\mathscr{V}_2(\epsilon(t)) + \mathcal{L}\mathscr{V}_3(\epsilon(t)). \tag{64}$$

$$\begin{aligned}\mathcal{L}\mathscr{V}_1(\epsilon(t)) &= 2e^T(t)P\left[\mathscr{A}\epsilon(t)+\mathscr{A}_1\epsilon(t-\tau(t))+\mathscr{A}_2F(\epsilon(t-\tau(t)))\right]\\&\quad+\text{trace}\left[(\mathscr{B}\hat{g}(t))^TP(\mathscr{B}\hat{g}(t))\right]+\epsilon^T(t)S_1\epsilon(t)\\&\quad-(1-\dot{\tau}(t))\epsilon^T(t-\tau(t))S_1\epsilon(t-\tau(t))\\&\le 2\epsilon^T(t)P\left[\mathscr{A}\epsilon(t)+\mathscr{A}_1\epsilon(t-\tau(t))+\mathscr{A}_2F(\epsilon(t-\tau(t)))\right]\\&\quad+\text{trace}\left[(\mathscr{B}\hat{g}(t))^TP(\mathscr{B}\hat{g}(t))\right]+\epsilon^T(t)S_1\epsilon(t)\\&\quad-(1-u)\epsilon^T(t-\tau(t))S_1\epsilon(t-\tau(t)).(u>0)\end{aligned} \tag{65}$$

$$\begin{aligned}\mathcal{L}\mathscr{V}_2(\epsilon(t)) &= \sum_{j=1}^{m}\epsilon^T(t-\tau_{j-1})Q_j\epsilon(t-\tau_{j-1})\\&\quad-\sum_{j=1}^{m}\epsilon^T(t-\tau_j)Q_j\epsilon(t-\tau_j),\end{aligned} \tag{66}$$

$$\begin{aligned}\mathcal{L}\mathscr{V}_3(e(t)) &= \sum_{j=1}^{m}\delta_j\dot{\epsilon}^T(t)R_j\dot{\epsilon}(t)\\&\quad-\sum_{j=1}^{m}\delta_j\int_{t-\tau_j}^{t-\tau_{j-1}}\dot{\epsilon}^T(s)R_j\dot{\epsilon}(s)ds.\end{aligned} \tag{67}$$

For any $t \geq 0$, there exists $k \in \{1, 2, \ldots, m\}$ such that $\tau(t) \in [\tau_{k-1}, \tau_k]$. When $j \neq k$, according to Lemma 1

$$\begin{aligned}
&-\delta_j \int_{t-\tau_j}^{t-\tau_{j-1}} \dot{\epsilon}^T(s) R_j \dot{\epsilon}(s) ds \\
&\leq \begin{bmatrix} \epsilon(t-\tau_{j-1}) \\ \epsilon(t-\tau_j) \end{bmatrix}^T \begin{bmatrix} -R_j & R_j \\ * & -R_j \end{bmatrix} \begin{bmatrix} \epsilon(t-\tau_{j-1}) \\ \epsilon(t-\tau_j) \end{bmatrix}.
\end{aligned}$$

When $j = k$, according to Lemma 1 and Lemma 2

$$\begin{aligned}
&-\delta_k \int_{t-\tau_k}^{t-\tau_{k-1}} \dot{\epsilon}^T(s) R_k \dot{\epsilon}(s) ds \\
&= -\delta_k \int_{t-\tau_k}^{t-\tau(t)} \dot{\epsilon}^T(s) R_k \dot{\epsilon}(s) ds \\
&\quad - \delta_k \int_{t-\tau(t)}^{t-\tau_{k-1}} \dot{\epsilon}^T(s) R_k \dot{\epsilon}(s) ds \\
&\leq -\max\{3W_{k1} + W_{k2}, W_{k1} + 3W_{k2}\},
\end{aligned}$$

where

$$W_{k1} = \begin{bmatrix} \epsilon(t-\tau(t)) \\ \epsilon(t-\tau_k) \end{bmatrix}^T \begin{bmatrix} -R_k & R_k \\ * & -R_k \end{bmatrix} \begin{bmatrix} \epsilon(t-\tau(t)) \\ \epsilon(t-\tau_k) \end{bmatrix},$$

$$W_{k2} = \begin{bmatrix} \epsilon(t-\tau_{k-1}) \\ \epsilon(t-\tau(t)) \end{bmatrix}^T \begin{bmatrix} -R_k & R_k \\ * & -R_k \end{bmatrix} \begin{bmatrix} \epsilon(t-\tau_{k-1}) \\ \epsilon(t-\tau(t)) \end{bmatrix}.$$

According to Definition 2 and the error dynamics, for any matrix S,

$$0 = 2\dot{\epsilon}^T(t) S^T \left\{ [\mathscr{A}\epsilon(t) + \mathscr{A}_1 \epsilon(t-\tau(t)) + \mathscr{A}_2 F(\epsilon(t-\tau(t))) - \dot{\epsilon}(t)]\, dt + \mathscr{B}\hat{g}(t) d\omega(t) \right\} \tag{68}$$

Applying (64)-(68) and Assumption (H6),

$$d\mathscr{V}(\epsilon(t)) = \mathcal{L}\bar{\mathscr{V}}(\epsilon(t))dt + 2[P\epsilon(t) + S\dot{\epsilon}(t)]^T \mathscr{B}\hat{g}(t) d\omega(t), \tag{69}$$

where the augmented operator is

$$\begin{aligned}
\mathcal{L}\bar{\mathscr{V}}(\epsilon(t)) &= \mathcal{L}\mathscr{V}(\epsilon(t)) + 2\dot{\epsilon}^T(t) S^T [\mathscr{A} e(t) + \mathscr{A}_1 e(t-\tau(t)) \\
&\quad + \mathscr{A}_2 F(\epsilon(t-\tau(t))) - \dot{\epsilon}(t)] \\
&\leq \xi^T(t) \hat{\Lambda} \xi(t) + \xi^T(t) \Gamma_1^T P \Gamma_1 \xi(t) \\
&\quad - \max\{3W_{k1} + W_{k2}, W_{k1} + 3W_{k2}\} \\
&\leq -\alpha \mathscr{V}(\epsilon(t)) + \beta \mathscr{V}(\epsilon(t-\tau(t))),
\end{aligned} \tag{70}$$

with

$$\xi(t) = \begin{bmatrix} \epsilon(t) \\ \epsilon(t-\tau_1) \\ \vdots \\ \epsilon(t-\tau_m) \\ \dot{\epsilon}(t) \end{bmatrix}.$$

Then

$$\begin{aligned}\mathbb{E}[\mathcal{L}\mathscr{V}(\epsilon(t))] &\leq \mathbb{E}\left[-\alpha\mathscr{V}(\epsilon(t)) + \beta\mathscr{V}(\epsilon(t-\tau(t)))\right] \\ &= -\alpha\mathbb{E}[\mathscr{V}(\epsilon(t))] + \beta\mathbb{E}[\mathscr{V}(\epsilon(t-\tau(t)))], \\ &t \in [t_k, t_{k+1}),\ i = \mathcal{S}(t_k) \in \mathbb{N}^+.\end{aligned} \tag{71}$$

Applying Lemma 4 to (71), there exists $\lambda_i > 0$ satisfying

$$\lambda_i - \alpha + \beta\epsilon^{\lambda_i \tau} = 0 \tag{72}$$

such that for $t \in [t_k, t_{k+1})$,

$$\mathbb{E}\{\mathscr{V}(\epsilon(t))\} \leq \mathbb{E}\{\mathscr{V}(\epsilon(t_k))\}\epsilon^{-\lambda_i(t_{k+1}-t_k)}. \tag{73}$$

For any time t, the expectation of the total Lyapunov functional $V(\epsilon(t))$ satisfies

$$\mathbb{E}[\mathscr{V}(\epsilon(t))] = \mathbb{E}[\mathscr{V}_1(\epsilon(t))] + \mathbb{E}[\mathscr{V}_2(\epsilon(t))] + \mathbb{E}[\mathscr{V}_3(\epsilon(t))]. \tag{74}$$

Using the bounds from Lemmas 7, 8 and 9, we obtain

$$\mathbb{E}[\mathscr{V}(\epsilon(t))] \leq \mu\mathbb{E}[\epsilon^T(t)P\epsilon(t)] + m, \tag{75}$$

where μ and m are defined in Theorem 1.

For $t \in [t_0, t_1)$ $(k = 0)$,

$$\begin{aligned}\mathbb{E}\{\mathscr{V}(\epsilon(t_1^-))\} &\leq \mathbb{E}\{\mathscr{V}(\epsilon(t_0))\}\epsilon^{-\lambda_i(t_1-t_0)} \\ \mathbb{E}\{\mathscr{V}(\epsilon(t_1^+))\} &\leq \mu\mathbb{E}\{\mathscr{V}(\epsilon(t_1^-))\} + m \\ &\leq \mu\mathbb{E}\{\mathscr{V}(\epsilon(t_0))\}\epsilon^{-\lambda_i(t_1-t_0)} + m\end{aligned} \tag{76}$$

For $t \in [t_1, t_2)$ $(k = 1)$,

$$\begin{aligned}\mathbb{E}\{\mathscr{V}(\epsilon(t_2^-))\} &\leq \mathbb{E}\{\mathscr{V}(\epsilon(t_1^+))\}\epsilon^{-\lambda_i(t_2-t_1)} \\ &\leq \mu\mathbb{E}\{\mathscr{V}(\epsilon(t_0))\}\epsilon^{-\lambda_i(t_2-t_0)} + m\epsilon^{-\lambda_i(t_2-t_1)} \\ \mathbb{E}\{\mathscr{V}(\epsilon(t_2^+))\} &\leq \mu\mathbb{E}\{\mathscr{V}(\epsilon(t_2^-))\} + m \\ &\leq \mu^2\mathbb{E}\{\mathscr{V}(\epsilon(t_0))\}\epsilon^{-\lambda_i(t_2-t_0)} + \mu m\epsilon^{-\lambda_i(t_2-t_1)} + m\end{aligned} \tag{77}$$

By mathematical induction, for $t \in [t_k, t_{k+1})$ $(k \geq 0)$,

$$\mathbb{E}\{\mathscr{V}(\epsilon(t_k^+))\} \leq \mu^k\mathbb{E}\{\mathscr{V}(\epsilon(t_0))\}\epsilon^{-\lambda_i(t_k-t_0)} + m\sum_{j=1}^{k}\mu^{k-j}\epsilon^{-\lambda_i(t_k-t_j)} \tag{78}$$

Assuming equally spaced impulses $(t_j = t_0 + jh)$,

$$\sum_{j=1}^{k}\mu^{k-j}\epsilon^{-\lambda_i(t-t_j)} = \epsilon^{-\lambda_i(t-t_0)}\sum_{j=1}^{k}\mu^{k-j}\epsilon^{\lambda_i jh} \tag{79}$$

Reindexing with $l = k - j$,

$$\begin{aligned}\sum_{j=1}^{k}\mu^{k-j}\epsilon^{\lambda_i jh} &= \sum_{l=0}^{k-1}\mu^l\epsilon^{\lambda_i(k-l)h} \\ &= \epsilon^{\lambda_i kh}\sum_{l=0}^{k-1}\left(\mu\epsilon^{-\lambda_i h}\right)^l\end{aligned} \tag{80}$$

Defining $r = \mu\epsilon^{-\lambda_i h}$ $(r \neq 1)$,

$$\sum_{l=0}^{k-1} r^l = \frac{1-r^k}{1-r} \tag{81}$$

Combining (79)-(81):

$$\begin{aligned}\mathbb{E}\{\mathscr{V}(\epsilon(t))\} \leq \mu^k \epsilon^{-\lambda_i(t-t_0)}\mathbb{E}\{\mathscr{V}(\epsilon(t_0))\} \\ + m\epsilon^{-\lambda_i(t-t_0)}\epsilon^{\lambda_i kh}\frac{1-r^k}{1-r}.\end{aligned} \tag{82}$$

For $t \in [t_k, t_{k+1})$,

$$k > \frac{t-t_0}{h} - 1 \tag{83}$$

implies

$$\mu^k \leq \mu^{\frac{t-t_0}{h}-1} = \mu^{-1}\epsilon^{\frac{\ln\mu}{h}(t-t_0)}. \tag{84}$$

Thus

$$\mu^k \epsilon^{-\lambda_i(t-t_0)}\mathbb{E}\{\mathscr{V}(e(t_0))\} \leq \mu^{-1}\exp\left[\left(\frac{\ln\mu}{h} - \lambda_i\right)(t-t_0)\right]\mathbb{E}\{\mathscr{V}(\epsilon(t_0))\}. \tag{85}$$

Under Assumption (H4) ($\lambda_i > \frac{\ln\mu}{h}$),

$$\begin{aligned}&\mu^k \epsilon^{-\lambda_i(t-t_0)}\mathbb{E}\{\mathscr{V}(\epsilon(t_0))\} \\ &\leq \mu^{-1}\epsilon^{-\alpha_i(t-t_0)}\mathbb{E}\{\mathscr{V}(\epsilon(t_0))\}\end{aligned} \tag{86}$$

where $\alpha_i = \lambda_i - \frac{\ln\mu}{h} > 0$.

For the second term, since $k \leq \frac{t-t_0}{h}$ and $r^k > 0$,

$$\begin{aligned}&\epsilon^{-\lambda_i(t-t_0)}\epsilon^{\lambda_i kh}\frac{1-r^k}{1-r} \\ &\leq \frac{m\epsilon^{-\lambda_i(t-t_0)}\epsilon^{\lambda_i kh}}{1-r} \\ &\leq \frac{m\epsilon^{\lambda_i(kh-(t-t_0))}}{1-r} \\ &\leq \frac{m}{1-r} \quad (\text{since } kh \leq t-t_0)\end{aligned} \tag{87}$$

Thus

$$m\epsilon^{-\lambda_i(t-t_0)}\epsilon^{\lambda_i kh}\frac{1-r^k}{1-r} \leq \frac{m}{1-\mu\epsilon^{-\lambda_i h}}. \tag{88}$$

Combining (86) and (88)

$$\mathbb{E}\{\mathscr{V}(\epsilon(t))\} \leq \mu^{-1}\epsilon^{-\alpha_i(t-t_0)}\mathbb{E}\{\mathscr{V}(\epsilon(t_0))\} + \frac{m}{1-\mu\epsilon^{-\lambda_i h}}. \tag{89}$$

As $t \to \infty$, the exponential term vanishes ($\alpha_i > 0$)

$$\limsup_{t\to\infty}\mathbb{E}\{\mathscr{V}(\epsilon(t))\} \leq \frac{m}{1-\mu\epsilon^{-\lambda_i h}}. \tag{90}$$

From (20), $\mathscr{V}(\epsilon(t)) \geq \eta\|\epsilon(t)\|^2$ with $\eta = \lambda_{\min}(P) > 0$, hence we obtain

$$\eta\mathbb{E}\{\|\epsilon(t)\|^2\} \leq \mathbb{E}\{\mathscr{V}(\epsilon(t))\}. \tag{91}$$

From (90), we have

$$\limsup_{t\to\infty}\mathbb{E}\{\|\epsilon(t)\|^2\} \leq \frac{m}{\eta(1-\mu\epsilon^{-\lambda_i h})}. \tag{92}$$

Based on Jensen's inequality, we have

$$\begin{aligned}\left\|\mathbb{E}\{\epsilon(t)\}\right\| &\leq \sqrt{\mathbb{E}\{\|\epsilon(t)\|^2\}} \\ &\leq \sqrt{\frac{m}{\eta(1-\mu\epsilon^{-\lambda_i h})}}.\end{aligned} \tag{93}$$

The proof is completed. □

Remark 5 In contrast to previous studies, which primarily focus on deception attacks under fixed or ideal timing conditions, this paper introduces a time-varying delay function into the attack model, significantly improving its practical relevance.Theorem 1 establishes a unified sufficient condition for the exponential convergence of the error system into the set $\mathcal{C}$, explicitly accounting for both time-varying delays and deception attacks via conditions (H1)–(H6). While earlier work focuses mainly on the attack pattern itself, Theorem 1 reveals that the attack type is merely one of several determining factors; the synchronization bound and convergence behavior also critically depend on the parameters embedded in the theorem. Furthermore, condition (H4) of Theorem 1 explicitly defines the exponential decay rate α_i for each mode, underscoring the role of the parameter α in controlling the convergence speed.

5 Simulations

A series of simulation experiments are carried out to validate the efficacy of the established theoretical results. A MASs consisting of six agents is considered, and the network topology is illustrated in Figure 2. The nonlinear dynamics of the six agents

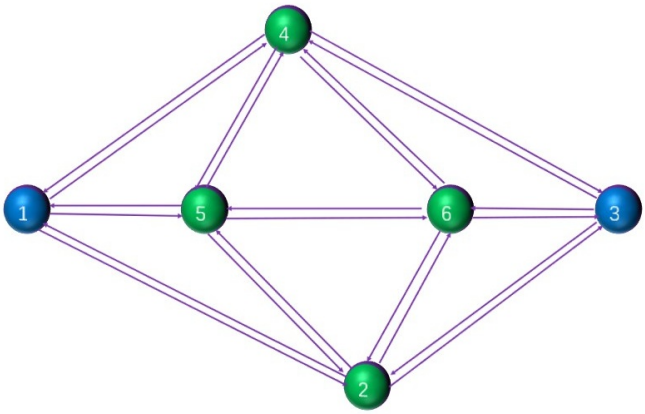

Fig. 2 The network topology of the MASs.

are given as following equation (94)

$$\begin{aligned} \mathrm{d}s_i(t) =& \Big(0.01s_i(t) + 0.03s_i\big(t-\tau(t)\big) + 0.01\sin\big(s_i\big(t-\tau(t)\big)\big) + u_i(t)\Big)\,\mathrm{d}t \\ &+ 0.01g\big(t, s_i(t), s_i\big(t-\tau(t)\big)\big)\,\mathrm{d}\omega(t) \end{aligned} \tag{94}$$

and the non-linear dynamic equation of the Leader is described as following equation (95)

$$\begin{aligned} \mathrm{d}l_o(t) =& \Big(0.01l_o(t) + 0.03l_o\big(t-\tau(t)\big) + 0.01\sin\big(l_o\big(t-\tau(t)\big)\big)\Big)\,\mathrm{d}t \\ &+ 0.01g\big(t, l_o(t), l_o\big(t-\tau(t)\big)\big)\,\mathrm{d}\omega(t) \end{aligned} \tag{95}$$

where $\tau(t) = 0.2 + 0.1\sin(0.5t)$.

Let $e_i(t)$ denote the tracking error $e_i(t) = s_i(t) - l_o(t)$. The Laplacian matrix L of the communication topology is computed as follows

$$L = \begin{bmatrix} 3 & -1 & 0 & -1 & -1 & 0 \\ -1 & 4 & -1 & 0 & -1 & -1 \\ 0 & -1 & 3 & -1 & 0 & -1 \\ -1 & 0 & -1 & 4 & -1 & -1 \\ -1 & -1 & 0 & -1 & 4 & -1 \\ 0 & -1 & -1 & -1 & -1 & 4 \end{bmatrix}$$

$D = \text{diag}[1, 0, 1, 0, 0, 0]$ is the pinning matrix.

Example 1 For this simulation, the static triggering constants are configured with the values $\bar{\beta} = 0.4$, $c = 5$, and $\epsilon = 0.1$. The relevant parameters required in Theorem 1 are taken as $\rho_M = 0.8123$ and $\mu = 0.8523$. Substituting these values into Theorem 1 yields $\lambda_1 = \lambda_2 = 30$, $\omega = 0.015$, and $h = h_1 = 0.16$. Moreover, we have $e^{-\alpha h^2} > \mu$, which strictly satisfies the positivity condition (H5). Together with the fulfilment of all other conditions (H1)–(H4) and (H6), the hypotheses of Theorem 1 are fully met, ensuring the exponential convergence of the error system into the set $\mathcal{C}$.

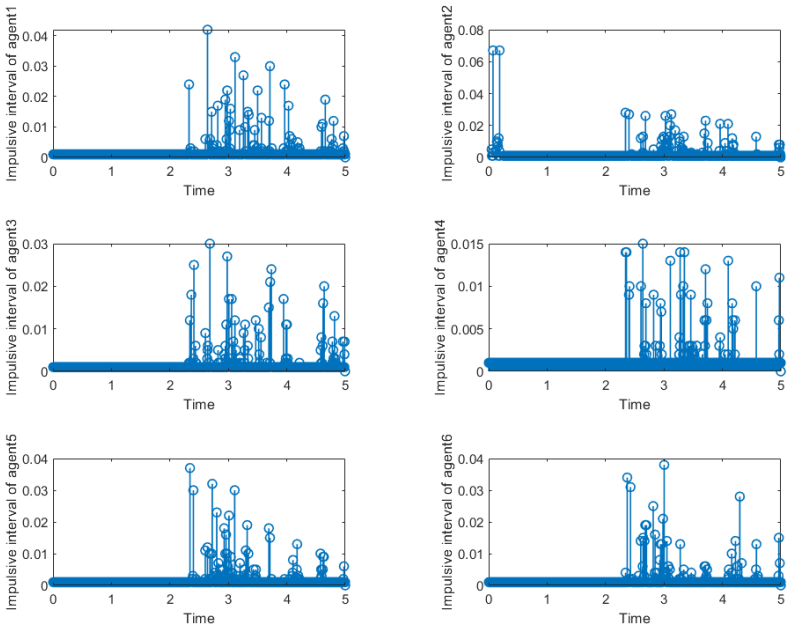

Fig. 3 Self-triggered time instants and sampling intervals for the six agents under Theorem 1.

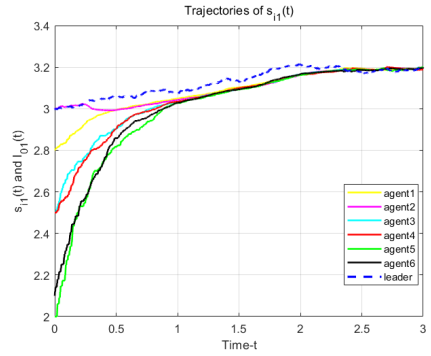

Fig. 4 Evolution under the static self-triggered mechanism stipulated by Theorem 1.

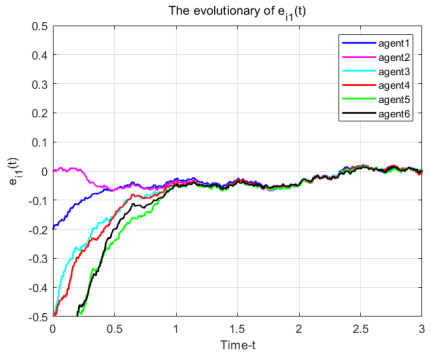

Fig. 5 Error evolution under the static self-triggered mechanism stipulated by Theorem 1.

Figure 3 shows the self-triggered instants and sampling intervals for the six agents when the conditions of Theorem 1 are satisfied. Figure 4 shows the evolutionary situation of s_{i1} and l_{01} under the static self-triggered mechanism. It can be observed that all follower agents successfully synchronize with the leader after a short transient period. The system trajectories confirm that the proposed control strategy ensures consensus despite communication constraints and external disturbances, demonstrating the robustness and practical applicability of the method.

As further validated in Figure 5, the norm of the tracking error $e_i(t)$ converges to a small neighborhood near zero. Specifically, the error converges to approximately 0.0084 at $t = 0.99\,\mathrm{s}$, which is significantly below the predefined threshold of 0.05. This rapid and stable convergence underscores the effectiveness of the proposed controller in achieving high-precision synchronization under the self-triggered communication scheme. The results clearly indicate that the overall system error converges uniformly and remains bounded, confirming the stability and consistency of the closed-loop system. Together, these findings provide strong support for the theoretical claims and demonstrate the practical viability of the proposed approach for multi-agent consensus.

Example 2 Suppose the static triggered parameters is $\bar{c} = 10$. Conditions of Theorem 1 are simultaneously violated under the current parameters. Conditions fail en masse: $\mu \approx 1.1 \times 10^3$ yields $r_i > 1$, negative $\alpha_i < 0$, and the impossible inequality $e^{-\alpha h_2} \leq 1$. Thus the convergence set $\mathcal{C}$ remains mathematically invalid.

Figure 6 shows self-triggered time instants and sampling intervals for the six agents beyond Theorem 1. As illustrated in Figures 7 and 8, the system achieves greater stability under the static self-triggered mechanism of Theorem 1. This stands in clear contrast to the performance degradation observed in Figure 8, where the error norm $||e_i(t)||$ exhibits sustained fluctuations under an invalid parameter configuration, and this directly substantiates that violating the theorem's conditions compromises system performance. This offers important insight into the robustness limitations of the control protocol and highlights the necessity of careful parameter tuning in real-world implementations.

As summarized quantitatively in Table 1, when the parameters meet the conditions of Theorem 1, the total number of triggering events is 18 851. In contrast, when the parameters violate Theorem 1, the number of triggers increases markedly to 49 809. This outcome directly

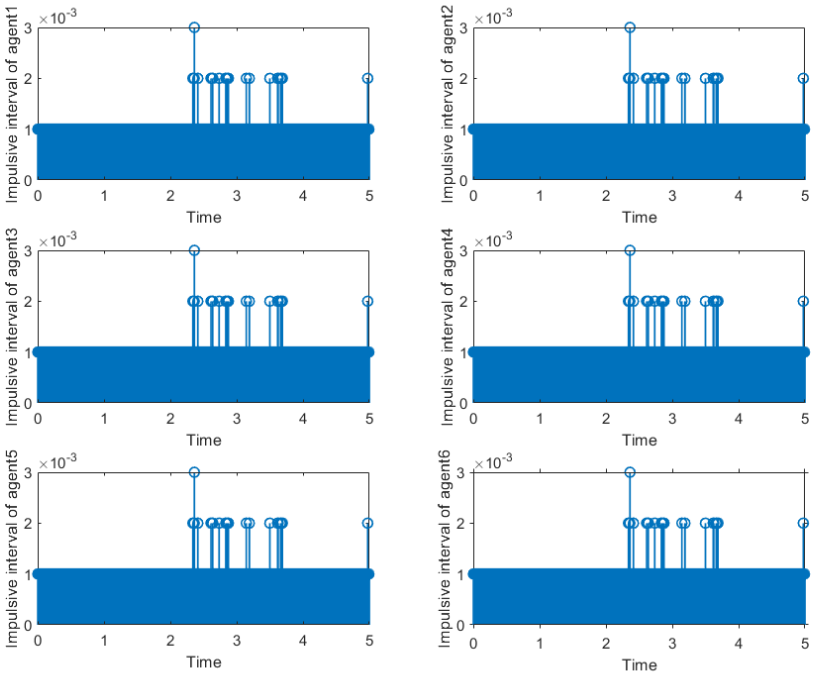

Fig. 6 Self-triggered time instants and sampling intervals for the six agents beyond Theorem 1.

supports the theoretical analysis: violation of the theorem's conditions results in mathematically invalid convergence properties and inefficient triggering performance. The noticeable degradation in triggering behavior under non-compliant parameters emphasizes the practical importance of Theorem 1 in reducing communication overhead.

Complying with Theorem 1 reduces the number of triggers by 30 958, equivalent to a 62.15% reduction, and improves communication efficiency by 30.59 percentage points. This considerable gain in resource utilization demonstrates the essential role of the theoretical results in designing efficient and practical self-triggered control systems for multi-agent networks. The findings strongly endorse the adoption of the proposed method in applications where communication resources are limited and operational efficiency is critical.

Table 1 Event-trigger counts for six followers. Tables should be placed in the main text near to the first time they are cited.

	F1	**F2**	**F3**	**F4**	**F5**	**F6**	**Total**
Conditions of Theorem 1	3345	2935	3087	3182	3104	3198	18851
Beyond Theorem 1	9958	9971	9970	9952	9958	9971	49809

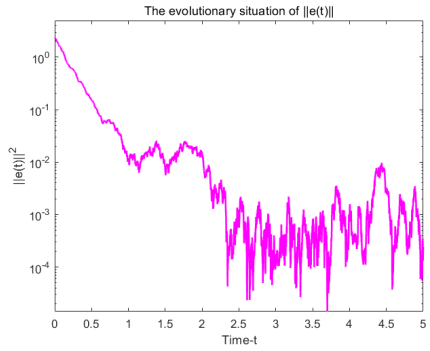

Fig. 7 Evolution under the static self-triggered mechanism stipulated by Theorem 1.

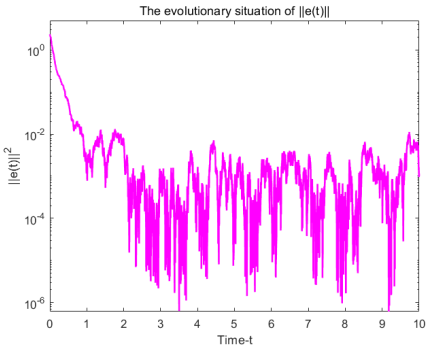

Fig. 8 Evolution under the static self-triggered mechanism beyond Theorem 1.

6 Conclusion

This study has tackled the mean-square bounded synchronization problem for multi-agent systems subject to dual-channel stochastic switching deception attacks with time-varying delays. This study has tackled the mean-square bounded synchronization problem for multi-agent systems subject to dual-channel stochastic switching deception attacks with time-varying delays. The proposed synchronization criteria have established verifiable conditions for achieving consensus under stochastic attacks. Numerical validation has confirmed that these verifiable conditions reduce triggering events. Future research has planned to investigate prescribed-time consensus under heterogeneous cyber-attacks and hybrid faults, with emphasis on adaptive dynamic event-triggered mechanisms for resilience-aware control. Continued investigation in these areas has aimed to deepen our understanding of complex multi-agent systems and advance the development of resilient control strategies for real-world applications.

Declarations

Funding Declaration

This research was funded by the Center for Research and Development of University Mathematics Teaching, Ministry of Education, China (Grant No. CMC20240633), the Natural Science Foundation of Anhui Province (Grant No. 2008085MG227), the Department of Education of Anhui Province (Grants No. 2023sx103, 2023AH040232, 2024fwxx051, 2023cxtd092, 2022cxtd162), and Tongling University (Grants No. 2023tlxypt05, 2022tlxyrc11, R23010, 2023tlxyrc39, 2024jxgl057, 2023xj078, 2023xj123, 2024tlxytyfzkt01).

Conflict of Interest

The authors declare that they have no conflicts of interest.

Ethics Declaration

Not applicable.

Consent for Publication

All authors have read and approved the final manuscript for publication.

Data Availability

All data generated or analyzed during this study are included in this published article [and its supplementary information files].

Materials Availability

Not applicable.

Code Availability

The custom code developed during this study is available from the corresponding author upon reasonable request.

References

[1] Lu R., Wu J., Zhan X., Yan H. Practical finite-time and fixed-time containment for second-order nonlinear multi-agent systems with IDAs and Markov switching topology. *Neurocomputing* **2024**, *573*, 127180.

[2] Kong M., Shen F., Du P., Peng X., Zhong W. Distributed secure consensus for multiagent systems based on removing intra-cluster coupling restrictions and its application to energy systems. *Information Sciences* **2024**, *653*, 150–165.

[3] Wang X., Cao Y., Niu B., Song Y. A novel bipartite consensus tracking control for multiagent systems under sensor deception attacks. *IEEE Transactions on Cybernetics* **2022**, to appear.

[4] Zhang D., Tang Y., Ding Z., Qian F. Event-based resilient formation control of multiagent systems. *IEEE Transactions on Cybernetics* **2019**, to appear.

[5] Zhang N., Chen G., Xia J., Park J., Xie X. Quantization-based adaptive fuzzy consensus for multiagent systems under sensor deception attacks: A novel compensation mechanism. *IEEE Transactions on Cybernetics* **2024**, to appear.

[6] Anand A., Guha D., Purwar S. Adaptive consensus control of leader-follower multi-agent system with actuator deception attacks. *Chaos, Solitons and Fractals* **2024**, *187*, 115344.

[7] Song W., You L., Li X. Stability of nonlinear time-varying systems with delayed stochastic impulses. *Communications in Nonlinear Science and Numerical Simulation* **2025**, *151*, 109120.

[8] Peng Q., Lin S., Tan M. Quantized hybrid impulsive control for finite-time synchronization of fractional-order uncertain multiplex networks with multiple time-varying delays. *Communications in Nonlinear Science and Numerical Simulation* **2025**, *142*, 108540.

[9] Hua C., Yang Z., Wang Y. Improved hierarchical stability criteria for time-varying delay systems with a novel matrix-valued polynomial negative determination lemma. *Journal of the Franklin Institute* **2025**, *362*, 107821.

[10] Wan Q., Chen W., Lu X. Secure consensus tracking of multi-agent systems with network-induced delays under deception attacks via guaranteed performance impulsive control. *Nonlinear Dynamics* **2023**, *111*, 12213–12232.

[11] Hu T., Zhang X., Shi K. Secure intermittent impulsive consensus control for fractional-order multiagent systems under denial-of-service and deception attacks. *Information Sciences* **2024**, *678*, 120949.

[12] Cao S., Yin Y., Li W., Liu Z., Chen Z. Time-varying formation control for heterogeneous multi-agent systems under actuator faults and deception attacks. *ISA Transactions* **2025**, to appear.

[13] Li W., Sader M., Zhu Z., Liu Z., Chen Z. Event-triggered fault-tolerant secure containment control of multi-agent systems through impulsive scheme. *Information Sciences* **2023**, *622*, 1128–1140.

[14] Zhao L., Yang G. Cooperative adaptive fault-tolerant control for multi-agent systems with deception attacks. *Journal of the Franklin Institute* **2019**, *357*, 3417–3432.

[15] He W., Gao X., Zhong W., Qian F. Secure impulsive synchronization control of multi-agent systems under deception attacks. *Information Sciences* **2018**, *459*, 354–368.

[16] Ni J., Zhao S., Cao J., Wang Z. Predefined-time consensus tracking of high-order multiagent system with deception attack. *Information Sciences* **2023**, *649*, 120–132.

[17] Wang X., Niu B., Shang Z., Niu Y. Distributed resilient adaptive consensus tracking control of nonlinear multi-agent systems dealing with deception attacks via K-filters approach. *Automatica* **2024**, *169*, 111871.

[18] Ma Y., Li Z., Xie X., Yue D. Adaptive consensus of uncertain switched nonlinear multi-agent systems under sensor deception attacks. *Chaos, Solitons and*

Fractals **2023**, *175*, 114022.

[19] Yuan X., Li Z., An T., Dong B. Double-layer game-based optimal event-triggered consensus control for stochastic multiagent systems against deception attacks. *Nonlinear Dynamics* **2024**, *113*, 1–17.

[20] Zhu Y., Liu H., Li C., Yu J. Consensus and security control of multi-agent systems based on set-membership estimation with time-varying topology under deception attacks. *International Journal of Control, Automation and Systems* **2022**, *20*, 3624–3636.

[21] Xiao J., Liu Y. Self-triggered consensus resilient control for multi-agent systems against sensor deception attacks based on a single parameter learning method. *Chaos, Solitons and Fractals* **2024**, *189*, 115649.

[22] Zheng L., Xu S. A periodic event-based approach to leader-following consensus for linear multi-agent systems with time-varying delays. *Journal of Systems Science and Complexity* **2025**, *38*, 805–820.

[23] Wen B., Huang J. Output feedback consensus for high-order stochastic multi-agent systems with unknown time-varying delays. *International Journal of Control, Automation and Systems* **2024**, *22*, 2823–2832.

[24] Yi C., Li J., Cai J., You Z., Jing C. Event-triggered synchronization for multi-agent networked systems with time-varying coupling strength and non-differentiable delays. *Mathematics and Computers in Simulation* **2025**, *236*, 12–28.

[25] Mathiyalagan K., Ma Y. K. Reliable stabilization of discrete-time nonlinear singular systems with time-varying delays. *International Journal of General Systems* **2024**, *53*, 949–970.

[26] Zhang K., Li Z. Y., Zhou B. Fully distributed output regulation of linear discrete-time multiagent systems with time-varying topology and delays. *Automatica* **2024**, *167*, 111755.

[27] Yang N., Fan X., Su H. Dynamic event-triggered delayed impulsive control for stochastic T-S fuzzy complex networks under cyber attacks. *Journal of the Franklin Institute* **2025**, *362*, 107863.

[28] Luo L., Li L., Cao J., Abdel-Aty M. Fractional exponential stability of nonlinear conformable fractional-order delayed systems with delayed impulses and its application. *Journal of the Franklin Institute* **2025**, *362*, 107353.

[29] Zhao Z., Zhang L., Yang S., Zhao N., Liu Y. Dual-triggered scheme for adaptive neural control of MIMO nonlinear switched systems against sensor and actuator attacks. *Communications in Nonlinear Science and Numerical Simulation* **2025**,

147, 108811.

[30] An Y., Liu Y., Wang H. Dual-channel triggered fuzzy adaptive output feedback control for uncertain nonlinear systems with deception attacks. *Chaos, Solitons and Fractals* **2025**, *191*, 115929.

[31] Ma K., He N., Fan Z. Resilient self-triggered predictive control for nonlinear system under dual-channel deception attacks. *Nonlinear Dynamics* **2024**, to appear.

[32] Chen X., Jia T., Wang Z., Xie X., Qiu J. Practical fixed-time bipartite synchronization of uncertain coupled neural networks subject to deception attacks via dual-channel event-triggered control. *IEEE Transactions on Cybernetics* **2023**, to appear.

[33] Zhang R., Li T., Guo L. Disturbance observer based H_∞ control for flexible spacecraft with time-varying input delay. *Advances in Difference Equations* **2013**, *2013*, 142.

[34] Boyd S., El Ghaoui L., Feron E., Balakrishnan V. Linear Matrix Inequalities in System and Control Theory. *SIAM Studies in Applied Mathematics* **1994**, Philadelphia, PA.

[35] Halanay A. Differential Equations: Stability, Oscillations, Time Lags. *Academic Press* **1966**, New York.

[36] Wang Z., Yuan J., Pan Y. Adaptive Second-Order Sliding Mode Control: A Unified Method. *Transactions of the Institute of Measurement and Control* **2018**, *40*, 1927–1935.

[37] He J., Guo X., Chen Z., Ren J. Adaptive distributed impulsive synchronization control for multi-agent systems under switching deception attacks on dual channels. *IEEE Transactions on Network Science and Engineering* **2025**, *12*, 2797–2809.

[38] He W., Mo Z., Han Q.-L., Qian F. Secure impulsive synchronization in Lipschitz-type multi-agent systems subject to deception attacks. *IEEE/CAA Journal of Automatica Sinica* **2020**, *7*, 1326–1334.